JOURNAL OF GEOPHYSICAL RESEARCH, VOL. 115, F00A15, doi:10.1029/2009JF001281, 2010



# Transport on river networks: A dynamic tree approach

Ilya Zaliapin,[1] Efi Foufoula-Georgiou,[2] and Michael Ghil[3,4]

Received 30 January 2009; revised 25 November 2009; accepted 11 January 2010; published 18 June 2010.

[1] This study is motivated by problems related to environmental transport on river networks. We establish statistical properties of a flow along a directed branching network and suggest its compact parameterization. The downstream network transport is treated as a particular case of nearest neighbor hierarchical aggregation with respect to the metric induced by the branching structure of the river network. We describe the static geometric structure of a drainage network by a tree, referred to as the static tree, and introduce an associated dynamic tree that describes the transport along the static tree. It is well known that the static branching structure of river networks can be described by self-similar trees; we demonstrate that the corresponding dynamic trees are also self-similar, albeit with different self-similarity parameters. We report an unexpected phase transition in the dynamics of three river networks (one from California and two from Italy), demonstrate the universal features of this transition, and seek to interpret it in hydrological terms.

**Citation:** Zaliapin, I., E. Foufoula-Georgiou, and M. Ghil (2010), Transport on river networks: A dynamic tree approach, *J. Geophys. Res.*, *115*, F00A15, doi:10.1029/2009JF001281.

## 1. Introduction and Motivation

[2] The topology of river networks has been extensively studied over the past decades using the suite of quantitative methods developed in the pioneering works of *Horton* [1945], *Strahler* [1957], *Shreve* [1966], and *Tokunaga* [1978]. These authors found that the geometry of real river networks can be closely approximated by so-called self-similar trees (SSTs). Such trees can be completely specified by a small number of parameters; this specification facilitates the development of similarity metrics and scaling theories within and across river networks. As a result, stream-ordering schemes and statistical self-similarity concepts have been explored to a considerable extent [see *Jarvis and Woldenberg*, 1984; *Rodriguez-Iturbe et al.*, 1992; *Peckham*, 1995; *Rodriguez-Iturbe and Rinaldo*, 1997; *Sposito*, 1998; *Peckham and Gupta*, 1999; *Veitzer and Gupta*, 2000; *Dodds and Rothman*, 2000, and references therein].

[3] The connection between river network topology and the hydrologic response of a basin has also been extensively studied; see, for instance, the early work of *Surkan* [1969], *Kirkby* [1976], and *Rodriguez-Iturbe and Valdes* [1979], while *Gupta and Mesa* [1988], and *Rodriguez-Iturbe and Rinaldo* [1997] review the later developments. Apart from streamflow, the river network is also known to structure other processes operating on it, such as sediment bed load, grain size, nutrients, riparian vegetation, and the food web structure of aquatic organisms [e.g., *Sklar et al.*, 2006; *Benda et al.*, 2004a, 2004b; *Kiffney et al.*, 2006; *Lowe et al.*, 2006; *Muneepeerakul et al.*, 2006; *Power and Dietrich*, 2002; *Rice and Church*, 1998; *Rice et al.*, 2006; *Stewart-Koster et al.*, 2007; *Wohl et al.*, 2007]. The impact of such processes is of great interest from environmental, economic, and societal points of view.

[4] The development of a systematic framework within which to study dynamical processes on river networks remains of considerable theoretical and practical interest in hydrology, geomorphology, and river ecology. In this paper, we propose a new way of studying dynamical processes that operate on directed trees, which are commonly used to model river networks. Specifically, we introduce the concept of a "dynamic tree," which describes the directed transport along the links of a "static tree" that has a given topology and link length distribution, as well as other space- and time-dependent attributes.

[5] This dynamic tree is likely to have a different hierarchy and topology than the static one. For instance, some of the static-tree branches might be completely cut off, either due to a blockage that prevents transport along these branches or due to the absence of conditions that favor sediment or nutrient generation for downstream transport. In this and other cases, the structure of the dynamic tree will differ from that of the static one, and this difference might affect the scaling of fluxes that participate in defining the envirodynamics on the network of interest. In general, a static tree of a given Horton-Strahler order [*Horton*, 1945; *Strahler*, 1957] could become a dynamic tree of a lesser or higher order, depending on the dynamics acting on the tree.

[1]Department of Mathematics and Statistics, University of Nevada, Reno, Nevada, USA.
[2]Saint Anthony Falls Laboratory and National Center for Earth-surface Dynamics, Department of Civil Engineering, University of Minnesota, Minneapolis, Minnesota, USA.
[3]Geosciences Department and Laboratoire de Météorologie Dynamique, Ecole Normale Supérieure, CNRS, IPSL, Paris, France.
[4]Department of Atmospheric and Oceanic Sciences and Institute of Geophysics and Planetary Physics, University of California, Los Angeles, California, USA.


0148-0227/10/2009JF001281

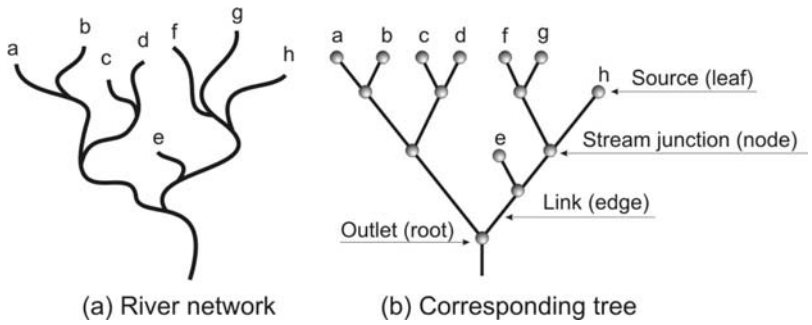


**Figure 1.** Tree representation of a river network: (a) hypothetical river network and (b) its representation by a binary tree. The network sources and the respective tree leaves are marked by the same letters. Figure 1 also illustrates the terminology used in our river transport study.

[6] The purpose of this paper is to study the dynamic topology of directed trees, starting with several simple cases, first synthetic and then realistic. We work here with downstream fluxes, oriented from the sources to the outlet, and with time-continuous transport. The possibility of reverse (upstream) motion, as in tidal systems or in association with the movements of biota, and discontinuous transport is left for future work. We focus on a dynamic hierarchy built on the concept of "connectivity": once two streams are connected, they both influence the downstream dynamics. In other words, a dynamic node of order 2 is created only when the fluxes from both order 1 streams do reach the connecting node. Such considerations will result in a different ordering of the dynamic tree than of the static one. Moreover, the newly created dynamic tree will be time oriented, a property that is absent in conventional static trees. Alternatively, one might keep track of traveled distance, rather than time: the two are equivalent if the flow velocity is constant along all the branches, which we will assume in the present paper, for simplicity sake.

[7] The static branching structure of river networks can be described by self-similar trees, following *Tokunaga* [1978], *Peckham* [1995], and *Peckham and Gupta* [1999], among others. It is shown here, using three actual river networks, that the corresponding dynamic trees are also self-similar, although their properties differ systematically from those of the corresponding static trees. We also demonstrate an unexpected phase transition in the dynamics on river networks, from a pattern of numerous disconnected fluxes initiated at the network sources to a single connected flux.

[8] Finally, we place our findings within the general framework of hierarchical aggregation and cluster dynamics. This framework helps describe and understand such diverse phenomena as population genetics, interacting particle systems in statistical mechanics, phylogeny, percolation, and extreme natural hazards.

[9] The paper is structured as follows. We review in section 2 the relevant concepts and main results in river network topology, including the branching taxonomies of *Horton* [1945] and *Strahler* [1957] and of *Tokunaga* [1978]. Section 3 introduces the concept of a dynamic tree that is associated with a given static tree, by using two examples from river transport. Hierarchical aggregation, including aggregation in an abstract metric space, is introduced in section 4. Section 5 describes the three river basins from California and Italy that we study here, as well as the static trees that represent the stream networks of these basins. The results of the study are presented in section 6. A summary and discussion, as well as an outline of further work follow in section 7. Examples of hierarchical aggregation from several fields of inquiry appear in Appendix A.

## 2. Network Topology: Overview of Concepts and Results

[10] This section summarizes the main concepts used in the topological analysis of river networks, as well as the key results of this analysis.

### 2.1. Branching-Order Taxonomies

[11] In our study of river transport, a drainage network is represented by a tree $\mathbb{T}$ (see Figure 1). In this representation, the stream junctions correspond to tree nodes, the stream segments between junctions correspond to links or edges, the network's sources correspond to tree leaves, and the basin outlet corresponds to the root of the tree. A source link is a link attached to a stream head; while an outlet link is the link attached to the basin outflow node.

[12] In many applications, there is a need to order the network links or tree edges according to their importance in forming the entire network. *Horton* [1945] developed a convenient way to order hierarchically organized river tributaries; this method was later refined by *Strahler* [1957] and further expanded by *Tokunaga* [1978]. Currently, the so-called Horton-Strahler (HS) and Tokunaga ordering schemes are standard tools of branching analysis, well beyond purely hydrological applications.

[13] Horton-Strahler ordering is performed in a hierarchical fashion, from the sources to the outlet. Each source link in a binary rooted tree is assigned an HS order $r$(source) = 1 (see Figure 2a). When two links with the same order $r$ meet, the link immediately downstream is assigned order $r + 1$; when two links with different orders meet, the link immediately downstream is assigned the larger one of the two orders [e.g., *Horton*, 1945; *Strahler*, 1957; *Newman et al.*, 1997]. A branch is defined as a union of connected links with the same order. We will denote by $N_r$ the total number of branches of order $r$. Notice that each branch has linear structure: each of its links can be connected to only one upstream and/or one downstream link from the same branch. The order $\Omega$

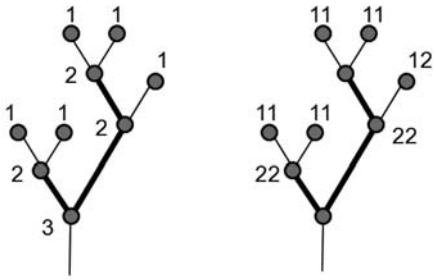


**Figure 2.** Example of (a) Horton-Strahler ordering and of (b) Tokunaga indexing of a static tree $\mathbb{T}_S$. Two order 2 branches are depicted by heavy lines. The Horton-Strahler orders refer, interchangeably, to the stream junctions or to the immediate downstream links. The Tokunaga indices refer to entire branches and not to individual links; these indices are shown next to the last downstream junction on each branch.

of a tree is the maximal order of its branches. An HS order can also be assigned to the stream junctions (tree nodes); in this case the order is the same as that of the immediate downstream link.

[14] Tokunaga indexing [*Tokunaga*, 1978; *Peckham*, 1995; *Newman et al.*, 1997] expands upon the Horton-Strahler orders; it is illustrated in Figure 2b. This indexing catalogues the merging points between branches of different order. A first-order branch that merges with a second-order branch is indexed by "12" and the total number of such branches is denoted by $N_{12}$. A first-order branch that merges with a third-order branch is indexed by "13" and the total number of such branches is $N_{13}$, and so on. In general, $N_{ij}$ for $j > i$ denotes the total number of order $i$ branches that join an order $j$ branch.

[15] The Tokunaga index $T_{ij}$ is the number of branches of order $i$ that merge with a branch of order $j$, normalized by the total number of branches of order $j$; in other words, $T_{ij}$ is the average number of branches of order $i < j$ per branch of order $j$:

$$T_{ij} = \frac{N_{ij}}{N_j}. \tag{1}$$

Merging of branches of different orders is referred to as side branching. A complete tree is one where side branching is absent. For incomplete trees, the side-branching indices become increasingly important as they help define a tree's structure and may help specify distinct classes of trees.

[16] For consistency, we denote the total number of order $i$ branches that merge with other order $i$ branches by $N_{ii}$ and notice that in a complete binary tree $N_{ii} = 2\ N_{i+1}$. The "diagonal" Tokunaga indices $T_{ii}$ thus satisfy

$$T_{ii} = \frac{N_{ii}}{N_{i+1}} \equiv 2.$$

The set $\{T_{ij}: 1 \le i \le \Omega - 1,\ 1 \le j \le \Omega\}$ of Tokunaga indices provides therewith a complete statistical description of the branching structure of an order $\Omega$ tree.

[17] We also use in this study the following two link statistics: the number of links within a given branch and the number $m_i$ of sources upstream from a link $i$. The latter statistic is also called a link's magnitude [*Shreve*, 1966]; a branch's magnitude is the magnitude of its furthest downstream link. The branch magnitude is coarsely proportional to the branch drainage area, with the coefficient of proportionality equal to the average drainage area for the stream sources. The average number of nodes and average magnitude of an order $r$ branch are denoted by $C_r$ and $M_r$, respectively.

### 2.2. Self-Similar Trees and Horton Laws

[18] The concept of self-similarity provides a powerful tool for describing and studying trees. A self-similar tree (SST) is defined by the constraint that the value of each Tokunaga index $T_{ij}$ depends only on the difference $(j - i)$ between the orders of respective branches. Accordingly, we define, for all $i$,

$$T_k := T_{i(i+k)} \ \text{ for } \ k = 1, 2, \ldots. \tag{2}$$

*Tokunaga* [1978] was probably the first to study SSTs; he assumed also that the ratio of two consecutive branching indices is constant:

$$\frac{T_{k+1}}{T_k} = c, \quad \text{or} \quad T_k = a\, c^{k-1} \ \text{ for } \ a, c > 0. \tag{3}$$

The SSTs that satisfy (3) are called Tokunaga trees.

[19] Empirically, the average values of branching statistics for observed river networks depend exponentially on the order $r$, for large $r$ and $\Omega$. In particular, for the total number $N_r$ of branches of order $r$, the average magnitude $M_r$, and the average number $C_r$ of links within an order $r$ branch we have

$$N_r = N_0\, R_B^{\Omega - r}, \quad M_r = M_0\, R_M^{r-1}, \quad C_r = C_0\, R_C^r, \tag{4}$$

for some positive constants $N_0$, $M_0$ and $C_0$. Such relationships are called Horton laws; the bases $R_B$, $R_M$, and $R_C$ of the exponential relationships are called stream ratios.

[20] *McConnell and Gupta* [2008] showed that the first two of the Horton laws (4) hold asymptotically, i.e., for $r \to \infty$, in a self-similar Tokunaga tree; they also proved that $R_B = R_M$. I. Zaliapin (manuscript in preparation, 2010) demonstrated asymptotic validity of all the laws in (4) and established the stream ratio inequality

$$R_C < R_B = R_M, \tag{5}$$

that had been conjectured by *Peckham* [1995]. In addition, I. Zaliapin (manuscript in preparation, 2010) showed that the Horton laws may or may not hold, under some additional assumptions on the Tokunaga indices $T_k$, for self-similar trees that do not necessarily satisfy condition (3).

## 3. Dynamic Versus Static Trees

[21] The topological structure of a river network is well described by a directed tree, which we denote by $\mathbb{T}_S$ and call the static tree. To describe the downstream transport on $\mathbb{T}_S$ we introduce the notion of a dynamic tree $\mathbb{T}_D$, which combines the topological structure of $\mathbb{T}_S$ with the corresponding

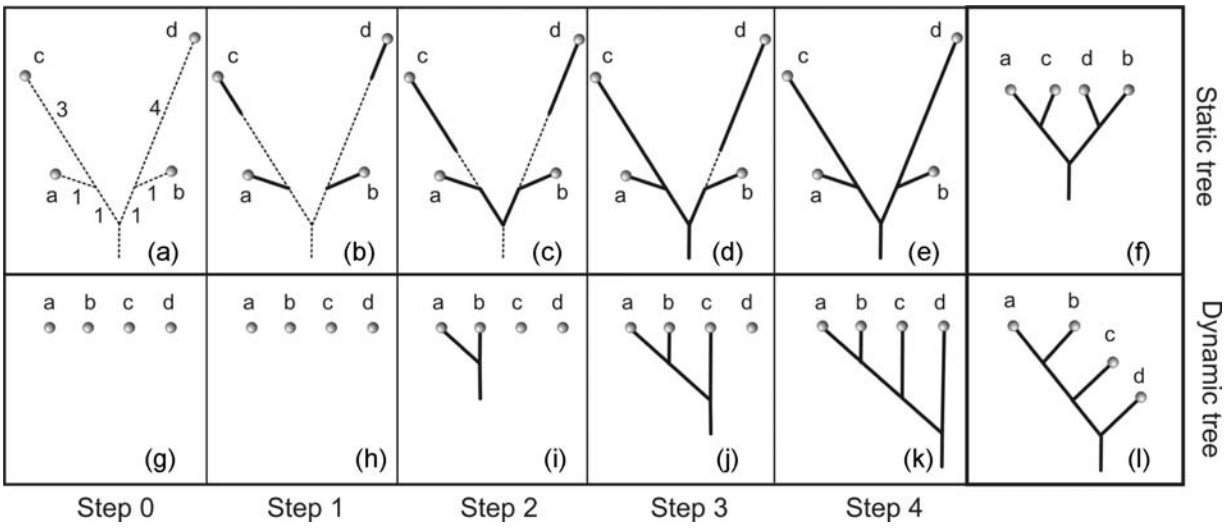


**Figure 3.** Constructing a dynamic tree $\mathbb{T}_D$. The initial static tree $\mathbb{T}_S$ and the final dynamic tree $\mathbb{T}_D$ are shown in Figures 3f and 3l. The dynamic tree reflects the propagation of a flux from the sources to the outlet of the static tree, at a constant velocity. (a–f) The static tree at different steps of this process; for visual convenience we explicitly show the static tree's link lengths. (g–l) The corresponding phases of the dynamic tree. Figure 3a indicates the lengths of the links in the static tree; each step takes one time unit, that is the flux propagates one unit of length downstream. See section 3.1 for details.

link length values. The dynamic tree is introduced as follows. Imagine that we inject a dye simultaneously into all the sources of our river network $\mathbb{T}_S$, and the dye starts propagating down the river, from the sources to the outlet, with the same constant velocity along all the streams. The influx of the dye is continuous and happens at a constant rate. The tree $\mathbb{T}_D$ describes the time-dependent history of the mergings of the colored streams.

[22] We consider below two detailed examples to further clarify this concept, while restricting ourselves to the simplest case of constant velocity along all the streams. Taking this velocity to be unity allows one to interchange time and length scales. We shall see that the dynamic tree $\mathbb{T}_D$ is completely determined by the static tree $\mathbb{T}_S$ and the set of time delays $\tau_i$ necessary for the dye to propagate from a junction $i$ to the nearest downstream junction. These delays can be proportional to the link lengths, as is the case in the present study, or be determined by spatially or temporally variable velocities. The latter extension is left for a future study.

### 3.1. Synthetic Example

[23] Figure 3 shows how to construct the dynamic tree for a basin with four sources: a, b, c, and d. The static tree for this basin is a complete binary tree shown in Figure 3f. The same tree with the link lengths explicitly displayed is shown in the Figures 3a–3e; Figure 3a indicates the values of these lengths.

[24] The consecutive phases of construction of the dynamic tree are shown in Figures 3g–3l. At step 0 (Figures 3a and 3g), all the links in the tree are "empty" (dashed lines) and the dye is injected into sources a, b, c, and d. Accordingly, we have four disconnected clusters of colored flux; they correspond to four disconnected nodes in Figure 3g. We assume that the dye is being continuously injected at all later times at a constant rate. Each step is a snapshot of this process after a unit time interval; recall that we use only constant velocity in this paper and, without loss of generality, this velocity equals unity.

[25] At step 1 the dye has propagated a unit length along each stream, which is depicted by solid lines in Figure 3b. Since all four streams are disconnected so far, the dynamic tree still consists of four disconnected branches, each of which corresponds to a colored stream of unit length. At step 2 the streams a and b merge, and so the nodes a and b are now connected into a single cluster in the dynamic tree. Notice that sources a and b are not directly connected in the static tree; this connection reflects a property of the dye's downstream propagation.

[26] At step 3 stream c reaches stream a. Since stream a by that time is already merged with stream b, we say that the stream c merges with the cluster of streams a and b; this is reflected in the dynamic tree in Figure 3j. Hence, at step 3 there exist two connected clusters of the colored flux: one cluster is formed by streams a, b, and c, while stream d alone forms the second cluster. Finally, at step 4, all the colored fluxes have merged. The conventional representation of both static and dynamic trees, which does not show the link lengths, is given in Figures 3f and 3l.

[27] This example shows that the dynamic tree $\mathbb{T}_D$ can be very different from the corresponding static tree $\mathbb{T}_S$. We notice in particular that in this example the static tree is a tree with no side branching; it has the largest possible Horton-Strahler order, $\Omega = 3$, for a tree with four sources. At the same time, the dynamic tree exhibits exhaustive side branching; accordingly, it has the smallest possible order, $\Omega = 2$, for a tree with four sources.

### 3.2. Data-Based Hydrologic Example

[28] We illustrate here the dynamic tree for an order 3 subbasin of the Upper Noyo basin. This basin is located in Mendocino County, California; it is described by *Sklar et al.* [2006] and appears in Figure 7a of section 5, along with an

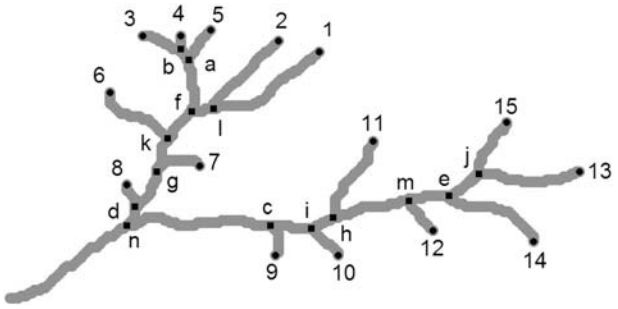


**Figure 4.** Stream network for an order 3 subbasin of the Noyo river, Mendocino County, California. The location of this subbasin is shown in Figure 7a; sources are marked by numbers (1 to 15), and stream merging points are marked by letters (a to n). The same marks are used in Figure 5, which shows both the static and the dynamic tree for this subbasin.

outline of the subbasin discussed in the present example. The stream network for this subbasin is shown in Figure 4; its fifteen sources are marked by numbers 1 to 15 and fourteen stream junctions by letters a to n. The static tree $\mathbb{T}_S$ for this stream network is shown in Figure 5a; it has the Horton-Strahler order $\Omega = 3$.

[29] The time-oriented dynamic tree $\mathbb{T}_D$ is shown in Figure 5b against the distance traveled by the dye from each source (on the ordinate). Notice that distance in Figure 5b can also be interpreted as time. The order of the dynamic tree is $\Omega = 4$. In this example (unlike the synthetic example of Figure 3), the dynamic tree shows a smaller degree of side branching compared to the static tree; this smaller degree yields a larger HS order. We shall see in other realistic examples, further below, that this seems to be the case for most actual river networks. Three snapshots of the simulated dye propagation, at distances $d = 20$, 200, and 600 are shown in Figure 6 to further illustrate the dynamic tree concept.

## 4. Dynamics of Hierarchical Aggregation

[30] The consecutive merging of river streams discussed in section 3 gives rise to a time-oriented dynamic tree. Study of such trees calls for the development of a new mathematical framework: hierarchical aggregation is a promising candidate for such a framework.

### 4.1. Hierarchical Aggregation

[31] Hierarchical aggregation studies how multiple individual particles (molecules, species, individuals, etc.) merge (aggregate, collide) with each other to form clusters in different physical, chemical, biological, or sociological settings [*Albert and Barabasi*, 2002; *Leyvraz*, 2003; *Wakeley*, 2009]. In the river transport setting, particles represent individual channel links, merging refers to the situation of two channels joining downstream, and a cluster represents all the upstream channels that jointly contribute to the flow at a given junction.

[32] Formally, consider a process that starts at time $t = 0$ with $N$ individual particles (say the sources of a river network), which can be considered as clusters of unit mass. As time evolves (and as a substance propagates down the river network) the clusters start to merge with one another, according to a set of rules imposed by the dynamics of propagation, thus forming consecutively larger clusters. If we assume that only two clusters can merge at the same time, then the number of clusters decreases by one after each merging. The process continues until all particles have merged into a single cluster of mass $N$; in our case, this would be when all the nodes of the river network are parts of the same cluster, i.e., when the whole system is connected.

[33] The evolution of the above process can be described by a time-oriented binary tree, whose leaves correspond to the initial particles, the root to the final cluster of $N$ particles, and each internal node to an intermediate cluster. Among the many instances of the above general aggregation scheme, we mention population genetics [*Wakeley*, 2009], phylogenetic trees [*Maher*, 2002], percolation [*Albert and Barabasi*, 2002; *Zaliapin et al.*, 2005], and billiards [*Gabrielov et al.*, 2008]; see Appendix A for details. *Bertoin* [2006] gives a modern review of mathematical results related to aggregation.

[34] An important role in aggregation studies is played by the notion of cluster dynamics [*Bogolyubov*, 1960; *Sinai*, 1972]. This concept refers to a system that contains an infinite number of interacting particles, which can be decom-

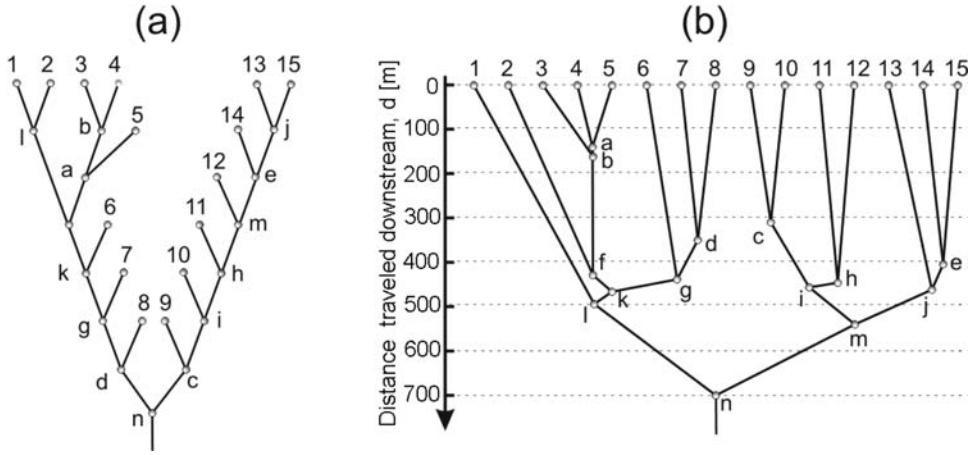


**Figure 5.** The static and the dynamic tree for the Noyo subbasin of Figure 4. (a) Static tree $\mathbb{T}_S$ and (b) dynamic tree $\mathbb{T}_D$. Letter and number markings are the same as in Figure 4.

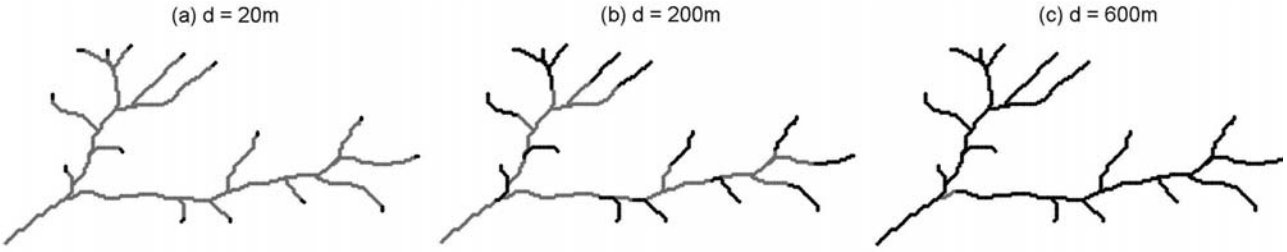


**Figure 6.** Three snapshots of the evolution of the dynamic tree (heavy solid lines) on the static tree (light solid lines) for the stream network of Figure 4.

posed into finite clusters that move independently of each other for some random interval of time. After this time, the particle interactions give rise to infinite range correlations (meaning that the mean cluster size becomes infinite, or an infinite number of particles affects each other's dynamics), although the system can be decomposed into yet another set of finite independent clusters, and so on.

[35] *Sinai* [1972, 1974] developed a self-consistent mathematical formalism and proved the existence of cluster dynamics for some particle systems in statistical mechanics. The ideas of cluster dynamics have been applied to plasma physics, economics, and the study of precursory patterns for extreme events in geophysics [*Rotwain et al.*, 1997; *Molchan et al.*, 1990; *Keilis-Borok and Soloviev*, 2003]. Recently, *Gabrielov et al.* [2008] evaluated numerically the cluster dynamics of elastic billiards, leading to the detection of what appear to be the first genuine phase transitions and scaling phenomena with time, rather than usual temperature $T$ or density, being the order parameter. Thus, a transition occurs and scaling develops as time $t$ approaches a critical value $t^*$, rather than as the parameter $T$ crosses a critical value $T^*$. As will be shown in section 6.2, we report here a remarkably similar and equally unexpected phase transition, with time being the order parameter, in the cluster dynamics of a river network.

### 4.2. Nearest Neighbor Clustering

[36] Hierarchical aggregation can be described in great generality by using the framework of nearest neighbor clustering in a metric space. Specifically, consider a finite set $\mathbb{S}$ with distance $d(a, b)$ for $a, b \in \mathbb{S}$; the elements of the set will be called points. The distance $d(A, B)$ between two subsets of points $A = \{a_i\}_{i=1,\dots,N_A}$ and $B = \{b_i\}_{i=1,\dots,N_B}$ from $\mathbb{S}$ is defined as the shortest distance between the elements of the sets:

$$d(A,B) = \min_{1\le i\le N_A, 1\le j\le N_B} d(a_i, b_j).$$

[37] Nearest neighbor clustering is a process that combines points from $\mathbb{S}$ into consecutively larger subsets, called clusters, by connecting at each step the two nearest clusters; this process can be described by the nearest neighbor spanning tree $\mathbb{T}$. Specifically, consider $N$ points $c_i^0 \in \mathbb{S}$, $i = 1,\dots, N$ with pairwise distances $d_{ij}^0 \equiv d(c_i^0, c_j^0)$. These points, considered as clusters of unit mass ($m_i = 1$), form $N$ leaves of the tree $\mathbb{T}$. Each node in this tree is assigned a time mark, thus producing a time-oriented tree; the leaves are assigned the time mark $t = 0$. Recall that in this work we focus on the constant velocity transport and thus use the time and distance interchangeably. Accordingly, one can talk about a distance-oriented tree $\mathbb{T}$ with distance marks being equal to the time marks. The first internal tree node is formed at the time $t_1 = \min_{ij} d_{ij}^0$ by merging two closest points $c_{i^*}^0$ and $c_{j^*}^0$ with $(i^*, j^*) = \mathrm{argmin}_{ij}\, d_{ij}^0$, where $\mathrm{argmin}_{ij} f(i, j)$ is defined as a pair $(i^*, j^*)$ such that $f(i^*, j^*) = \min_{ij} f(i, j)$. This merging creates a new cluster of two points, with a mass of $m_i + m_j = 2$. Hence, at time $t_1$, there exist $N - 1$ clusters: $N - 2$ clusters with unit mass and one cluster of mass $m = 2$.

[38] We can now reindex so as to work with clusters $c_i^1$, $i = 1,\dots, N - 1$; their total mass is $\sum_{i=1}^{N-1} m_i = N$ and pairwise distances are $d_{ij}^1 \equiv d(c_i^1, c_j^1)$. The second internal node of tree $\mathbb{T}$ is formed at time $t_2 = \min_{ij} d_{ij}^1 > t_1$ by merging the two closest clusters from the set $\{c_i^1\}_{i=1,\dots,N-1}$. Thus, at time $t_2$ we have $N - 2$ clusters $c_i^2$ such that their total mass is $N$ and pairwise distances are $d_{ij}^2 \equiv d(c_i^2, c_j^2)$. We continue in the same fashion, so the $k$th internal cluster, for $1 \le k \le N-2$, is formed at time $t_k = \min_{ij} d_{ij}^k > t_{k-1}$, and at that time we have $(N - k)$ clusters $c_i^k$, $i = 1, \dots, N - k$ with masses $m_i$ such that $\sum_{i=1}^{N-k} m_i = N$. Finally, at time $t_{N-1}$ we create a single cluster of mass $N$ that combines all points $c_i^0$; this cluster forms the root of the tree $\mathbb{T}$.

[39] Consider two nodes $a$ and $b$ from the nearest neighbor tree and let $t_a$ and $t_b$ be their time marks; recall that the tree is time oriented by the definition of the successive times $t_k = \min_{ij} d_{ij}^k > t_{k-1}$ at which the cluster mergers occur. The ancestors of a node are its parent, the parent of that parent, and so on, all the way to the root. Clearly, the time mark for an ancestor is larger than that of a descendant. The nearest common ancestor $p$ of nodes $a$ and $b$ is their common ancestor with the minimal time mark $t_p$.

[40] The distance $u(a, b)$ along the nearest neighbor tree is defined as the maximum of the values $u(a, p) \equiv t_p - t_a$ and $u(b, p) \equiv t_p - t_b$. This distance satisfies two of the usual distance axioms, symmetry and strict positivity, but the triangle inequality can be replaced by a more stringent one, namely

$$u(a,b) \le \max\,[u(a,c),\, u(c,b)],$$

which holds for any three nodes $a$, $b$ and $c$. Such a distance function is called an ultrametric [*Rammal et al.*, 1986; *Schikhof*, 2007]. Ultrametric spaces have many peculiar properties; for instance, one can rename any triplet $a$, $b$, $c$ of nodes in such a way that

$$u(a,c) = u(b,c).$$

These unusual properties give ultrametric spaces considerable flexibility in applications, and point sets connected via nearest neighbor clustering are a representative example of such spaces.

[41] In our river transport problem, the space $\mathbb{S}$ is the set of all river sources. The distance $d(a, b)$ between two sources is defined as the time necessary for the corresponding fluxes injected into these two sources to meet down the river path. If the static river geometry is described by the tree $\mathbb{T}_S$ (and we assume, as previously stated, that fluxes move downstream continuously with unit speed) the distance $d(a, b)$ between two sources equals the maximal length along the tree to their nearest common parent in $\mathbb{T}_S$. The nearest neighbor spanning tree of hierarchical aggregation theory thus becomes what we called so far, in the context of river transport, the dynamic tree $\mathbb{T}_D$.

[42] As previously stated, this dynamic tree differs, in general, from the static tree $\mathbb{T}_S$ and depends not only on the topology of the latter, but also on the actual length of the links. The ultrametric distance $u(a, b)$ equals the time necessary for the above-mentioned fluxes to belong to the same cluster or, equivalently, the time to establish a connected colored path between sources $a$ and $b$. If the velocities vary in time or space, then the spanning tree $\mathbb{T}_D$ will depend on the specific dynamics of the processes operating on the static tree. To better understand transport on river networks, we elucidate in sections 5 and 6 the connection between the statistical properties of $\mathbb{T}_S$ and those of $\mathbb{T}_D$ by using three real river networks.

## 5. River Basin Data

[43] We have analyzed three river basins: Upper Noyo, Mendocino County, California (called here Noyo); Tirso, Sardinia, Italy; and a part of the Brenta basin at the confluence with the Grigno river, Trento, Italy (called here Grigno). Information about the physiographic and geologic characteristics of these basins can be found in the work of *Sklar et al.* [2006], *Pinna et al.* [2004], and *Guzzetti et al.* [2005], respectively. In our analysis we used Digital Elevation Models (DEMs) with regularly gridded pixel resolutions of 10 m for the Noyo basin, 30 m for the Grigno basin, and 100 m for the Tirso basin.

[44] In an actual landscape, channels are initiated when the area upstream suffices to create a sustainable source of streamflow and this source imprints a permanent channel on the terrain. Although these channels are typically detectable by field observations, the extraction of the channel initiation points, or "channel heads," from DEMs has been a subject of sustained effort [e.g., *Montgomery and Dietrich*, 1989; *Tarboton et al.*, 1991; *Montgomery and Foufoula-Georgiou*, 1993; *Costa-Cabral and Burges*, 1994; *Giannoni et al.*, 2005; *Hancock and Evans*, 2006].

[45] In typical DEM analysis, channel heads are mapped where the upstream area, or (area) × (typical slope), exceed a given threshold; the parameters of such relationships are field calibrated. More recently, the availability of high-resolution, 1 m elevation data from light detection and ranging (lidar) has initiated a new generation of methodologies for the automatic detection of channels as terrain "features" [e.g., *Lashermes et al.*, 2007; *Passalacqua et al.*, 2010]. Given the available DEM resolution, and the fact that the focus of this study is not the extraction of the most accurate river network from the available DEMs, we adopted a simple criterion for channel initiation as $A_c = 100$ pixels for all three basins. This criterion is certain to miss the smallest first order basins in the Tirso basin but the extracted network, although clipped in its uppermost branches, still has the right topology.

[46] The extracted stream networks for the three river basins (using the steepest gradient D8 algorithm) are shown in Figure 7. The corresponding dynamic stream networks were then constructed for each basin, assuming a constant unit speed of downstream propagation for the fluxes. We thus analyzed two different kinds of trees, static and dynamic, for each basin.

## 6. Branching Characteristics of River Networks

[47] In this section we quantify similarities and differences between the branching topology of static and dynamic trees and demonstrate a phase transition phenomenon in the dynamics of river networks.

### 6.1. Self-Similarity Indices

[48] Figure 8 shows the distributions of the number $N_r$, average magnitude $M_r$, and the average number $C_r$ of links for branches of order $r$ for the static trees (Figures 8a and 8b) and dynamic trees (Figures 8c and 8d) of the three basins.

[49] Despite the usual small sample fluctuations, Figure 8 demonstrates a large degree of consistency among the branching indices. All branching statistics considered are closely approximated by the Horton laws. Moreover, these results suggest that the relationship (5) holds in all the cases considered herein.

[50] We observe that the values of the stream ratios for static trees are higher than the corresponding values for dynamic trees. This means that the degree of side branching (i.e., the proportion of network branches that merge with branches of a higher Horton-Strahler order) is larger for static trees than for dynamic trees.

[51] The only indices that deviate considerably from the Horton laws at higher orders are $C_r$ (the average number of nodes within an order $r$ branch) for the Noyo basin's static and dynamic trees; this discrepancy warrants further investigation. Apart from this point, we conclude that both types of trees, dynamic and static, can be closely approximated by Tokunaga SSTs; the characteristic indices, however, differ from one type to the other.

### 6.2. Phase Transition in Dynamic Trees

[52] Does river network connectivity, in terms of elements of the network participating in transport, exhibit a phase transition, with time being the order parameter, akin to those found in other systems? Figure 9 shows the fractional magnitudes $m_i/N$ of the branches in the dynamic trees as a function of the distance $d$ traveled by the dye. Recall that this distance can also be interpreted as the time $t$ when the node was created by merging of upstream branches.

[53] In Figures 9a, 9c, and 9e we observe the following scenario: We start at distance $d = 0$ (or time $t = 0$) with $N$ branches (clusters) of unit magnitude corresponding to the network sources. As distance increases (time evolves), the number of clusters decreases while their magnitudes become larger and exhibit substantial variability. In particu-

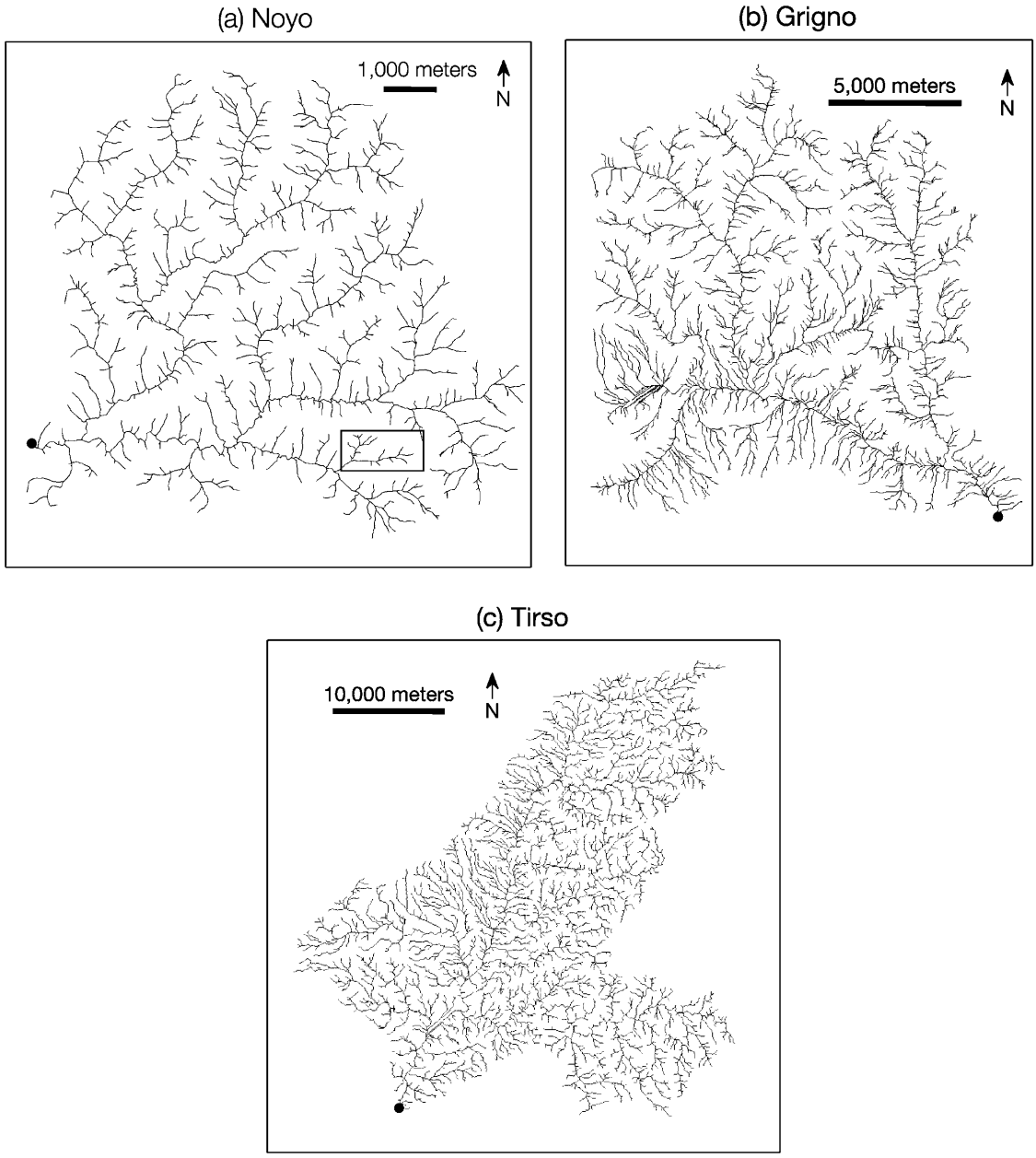


**Figure 7.** Stream networks of the three basins analyzed in this study shown as static trees; outlets are marked by black dots. (a) Upper Noyo basin, Mendocino County, California; the outlet is located at 39°26′N, 123°45′W, and the order 3 subbasin of Figures 4–6 is outlined by a small, light rectangle (i.e., southeastern). (b) A part of the Brenta basin, at the confluence with the Grigno river (called Grigno basin), Trento, Italy; the outlet is located at 40°00′04.96″N, 8°49′59.26″E. (c) Tirso, Sardinia, Italy; the outlet is located at 46°00′28.40″N, 11°38′ 21.55″E.

lar, at small distances the maximal magnitude increases exponentially with distance; this growth is reflected by an approximately linear form of an upper envelope of the points (envelope not shown). Furthermore, we notice that at short distances (small times) the magnitude distribution is "continuous;" that is, it does not have significant gaps. At some critical distance $d^*$ (time $t^*$), however, the distribution undergoes a marked qualitative change: a prominent maximal cluster appears, such that its magnitude becomes significantly larger than that of the second largest cluster. Moreover, while the magnitude of the largest cluster keeps growing, the rest of the distribution is fading off and so, after some time, all clusters present at $d = 0$ merge with the largest cluster. Still, at the critical distance $d^*$, the magnitude of the largest cluster is just about 10% of the total magnitude $N$ of the system, and this is the case for Figures 9a, 9c, and 9e.

[54] The magnitude distribution of the clusters was analyzed for $d$ varying from 0 to about $2d^*$, in both log-log and semilogarithmic scales (not shown). Our analysis strongly suggests that the magnitude distribution at smaller

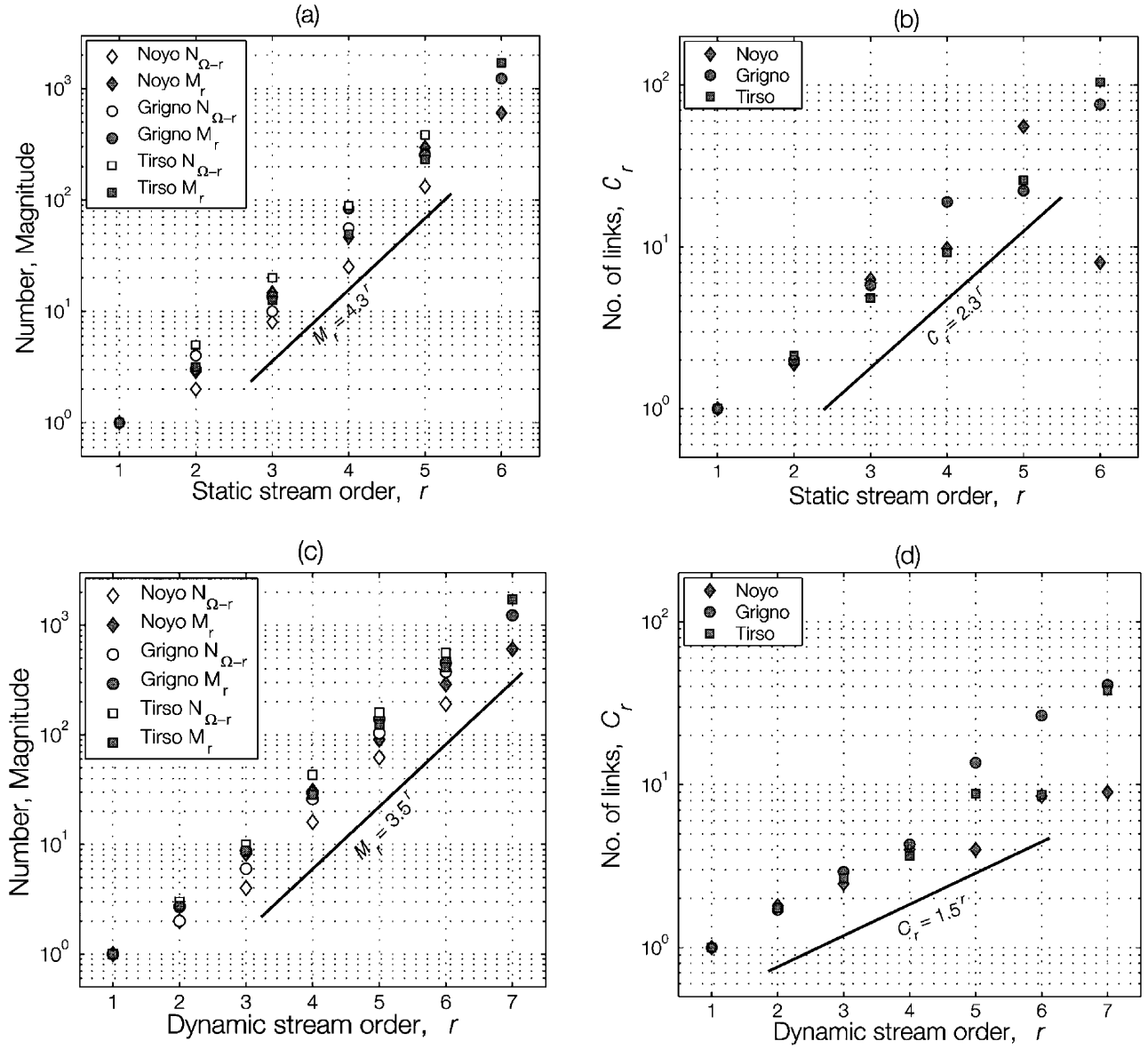


**Figure 8.** Branching statistics for the stream trees of the Noyo, Grigno, and Tirso basins, shown in Figure 7. (a and c) Number $N_r$ and average magnitude $M_r$ for the three static and the three dynamic trees and (b and d) average number $C_r$ of links within a branch for static and dynamic trees.

distances has an exponential tail, while at the critical distance $d^*$ it becomes a power law. This observation is illustrated in Figures 9b, 9d, and 9f, which show the magnitude distribution, in log-log coordinates, at the critical distance $d^*$ and at a shorter distance $d \approx d^*/2$; those distances are indicated by vertical lines in Figures 9a, 9c, and 9e. Recall that, in a log-log plot, power law behavior shows up as a straight line, while exponential behavior becomes a convex curve. This change indicates that a phase transition occurs at the distance $d^*$.

[55] This phase transition is further illustrated in Figure 10, which shows three snapshots of the dye propagating down the Noyo basin. The distances traveled by the dye at these snapshots are marked by vertical lines in Figure 11; the largest distance is chosen to be equal to the critical distance $d^*$ for this basin. Figure 11 shows the number of clusters (dotted line) and the magnitude of the largest cluster for the Noyo dynamic tree (solid line), as a function of downstream propagation distance. One can easily see how unconnected clusters suddenly merge together at the critical distance $d^* \approx$ 1000 m. Importantly, the value of critical distance is independent of the basin order; hence such a merging happens simultaneously at all the scales (basin orders), constituting a phase transition.

## 7. Concluding Remarks

### 7.1. Summary and Discussion

[56] In this study we have focused on the statistical description of environmental transport on river networks. We have approached the problem by considering downstream transport on such a network as a particular case of

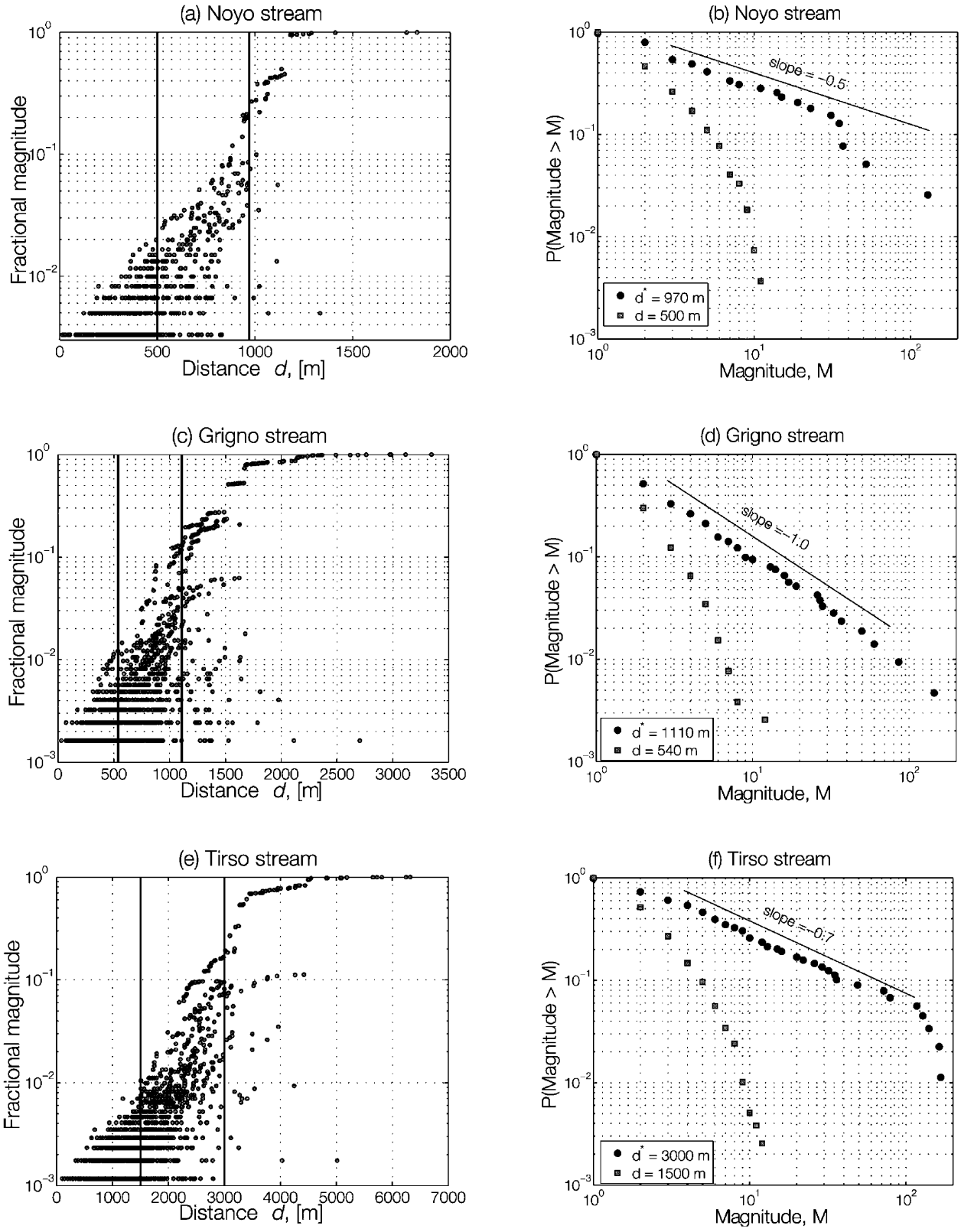


**Figure 9.** Phase transition in river network dynamics. (a, c, and e) Fractional branch magnitudes $m_i/N$ as a function of the distance $d_i$ traveled by the dye at the instant of branch creation. (b, d, and f) Distribution of branch magnitudes $m_i$ at the critical distance $d^*$ (circles) and at an earlier time, given by $d$ (squares), for the dynamic trees of the three basins. Each of these plots shows two distributions at distances $d^*$ and $d < d^*$, respectively; the corresponding distances are depicted by vertical lines in Figures 9a, 9c, and 9e. The downward deviations from pure power laws are due to the finite size effect.

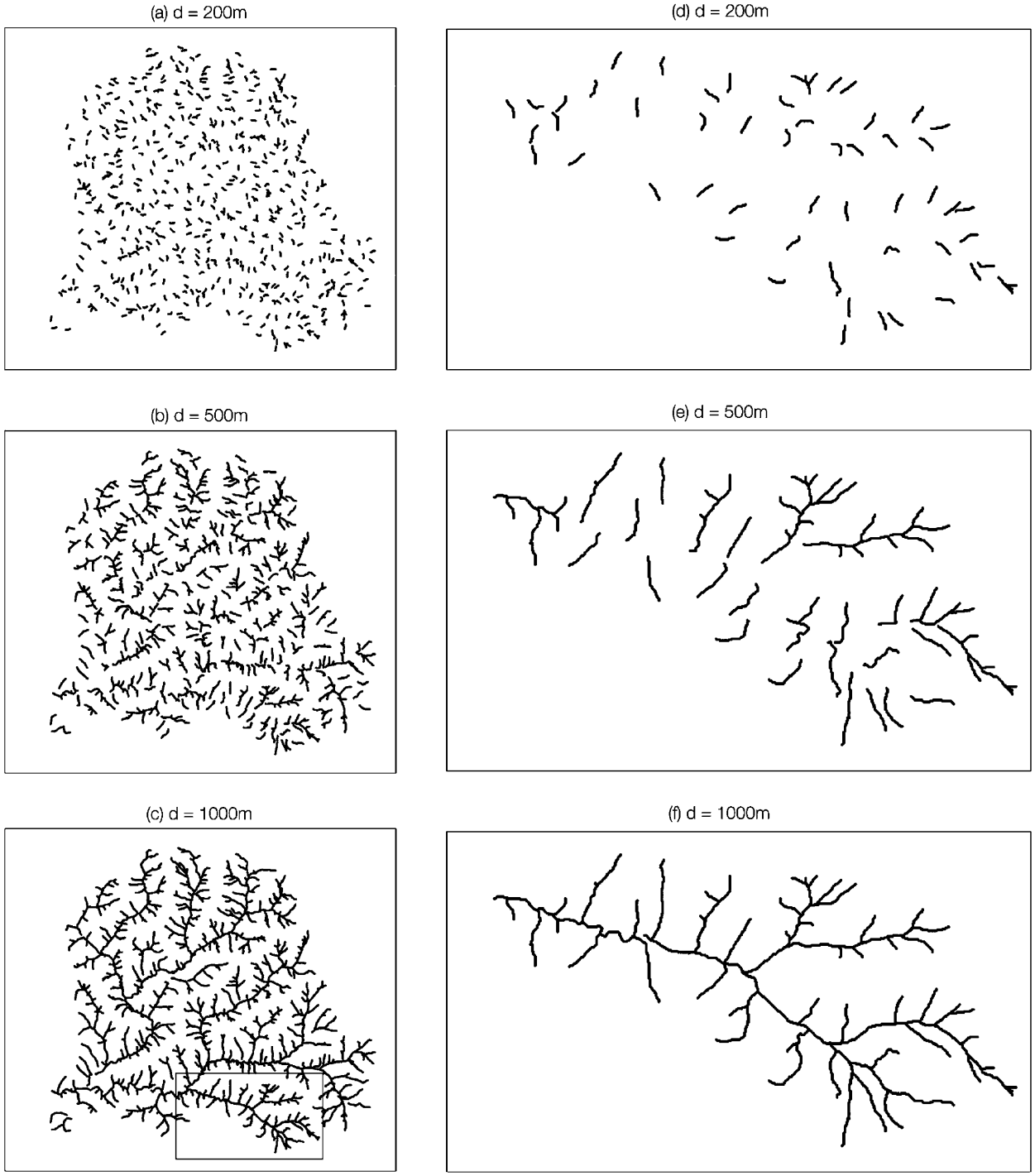


**Figure 10.** Transport down the Noyo stream network. Three snapshots of flux propagation from the stream sources to the outlet at (a and d) $d = 200$ m, (b and e) $d = 500$ m, and (c and f) $d = 1000$ m. Figures 10a–10c show the entire Noyo basin, while Figures 10d–10f zoom onto an order 4 subbasin located in the basin's southeastern part. This order 4 subbasin encompasses the order 3 subbasin shown in Figures 4–6; its location is depicted by a light rectangle in Figure 10c. See also Figure 11.

nearest neighbor hierarchical aggregation. The so-called ultrametric induced by the branching structure of the river network provides the distance function with respect to which the downstream flow gives rise to clusters that decrease in number and increase in size with time (see Figures 10 and 11).

[57] We have described the static topological structure of a river network by the type of tree structure that goes back to the pioneering studies of *Horton* [1945], *Strahler* [1957], and *Shreve* [1966]; this structure has been referred to as a static tree, to distinguish it from the associated dynamic tree

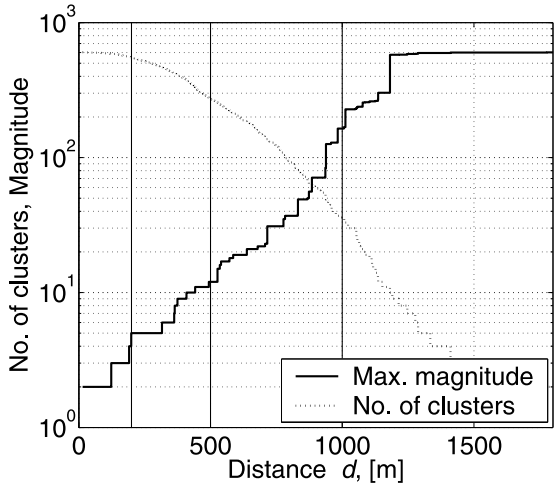


**Figure 11.** Cluster evolution for the Noyo basin downstream flux transport: number of clusters (dotted line) and largest cluster size (heavy solid line). Light vertical lines correspond to the three snapshots in Figure 10.

(section 3, Figures 3 and 5). The latter concept helps describe downstream transport along the static tree.

[58] We have studied the statistical properties of both static and dynamic trees using the Horton-Strahler and Tokunaga branching taxonomies. Using the DEM-extracted river networks in three river basins (Noyo, Grigno and Tirso) we have shown that both static and dynamic trees can be well approximated by Tokunaga self-similar trees (SSTs). The Horton-Strahler and Tokunaga parameters of these two types of trees differ significantly, though, for each of the three basins (section 6.1, Figure 8). This difference supports the relevance of the dynamic tree concept; its parameter values depict important properties of the envirodynamics on a given river network that are not captured by the conventional, static tree.

[59] An important new result of this study is the phase transition we have found in river network dynamics in section 6.2: as one fills an empty river network through its sources, or injects a dye at the sources of a water-filled one, the number of clusters of connected nodes decreases and the size of the largest cluster increases, until a dominant cluster of connected streams forms. During this process, the time-dependent size distribution of the connected clusters changes from an exponential to a power law function as the critical time approaches (Figure 9).

[60] This phenomenon, which may seem rather unexpected in the present hydrological setting, can be better understood within the framework of complex networks. This framework has been explored in many natural and socio-economic settings, ranging from the functioning of a cell to the organization of the Internet [*Albert and Barabasi*, 2002; *Dorogovtsev and Mendes*, 2002; *Newman*, 2003].

[61] The mathematical theory of complex networks considers a group of nodes that can be connected with each other according to some problem-specific rules, thus forming a graph. In the simplest case, the node connections are independent of each other and can be specified by the probability $p$ that two randomly chosen nodes are connected. There exists a critical value $p_c$ such that, for $p < p_c$, the network consists of isolated clusters, while a single giant cluster appears as $p$ crosses $p_c$, and spans the entire network. The same phenomenon is observed under more realistic rules of node connectivity as well. The appearance of the giant cluster is remarkably reminiscent of infinite cluster formation in percolation theory [*Stauffer and Aharony*, 1994].

[62] *Albert and Barabasi* [2002] review parallels and differences between complex network theory and percolation theory. The book by *Newman et al.* [2006] collects the major papers in complex network theory, while *Barrat et al.* [2008] provide an introduction for a readership of physicists, and *Durrett* [2007] gives a rigorous mathematical treatment of the topic.

[63] It readily follows from the analysis of section 3 that transport on river networks fits rather naturally the complex network paradigm. Formally, each stream source is represented by a node and two streams are considered to be connected when their respective fluxes join downstream. This is exactly the scheme we used to define a dynamic tree, with the only difference that we have ignored the connections between nodes within already formed clusters. This difference does not affect the process of cluster formation, so the results of the complex network theory do apply to envirodynamics on river networks. From this point of view, the rather sudden formation of the giant cluster and the corresponding transition of the cluster magnitude distribution from exponential to power law seems rather natural.

[64] There is an important difference, though, between complex networks in general and the dynamic trees considered in this study. Our dynamic trees, unlike general networks, are time oriented, i.e., their nodes can be ordered in "time" or with respect to a "downstream distance" parameter. The ultrametric distance along such trees satisfies a stronger triangle inequality than ordinary distance (see section 4.2), and thus induces interesting properties [e.g., *Schikhof*, 2007]. In fact, a set of points in a metric space with a traditional distance $d$ naturally forms an ultrametric tree according to the nearest neighbor clustering procedure described in section 4. As shown there, hierarchical aggregation via nearest neighbor clustering provides a common framework for many apparently different processes (such as billiards, river transport, and percolation) in the setting of ultrametric trees, and thus may provide novel insights into these processes.

[65] In percolation models, the cluster size distribution at phase transition is given by a power law whose index is a function of the system's dimension alone. In our three river networks, this index differs from one network to another (see Figures 9b, 9d, and 9f). We notice that in the hierarchical aggregation on dynamic trees, different clustering rules may correspond to different effective "dimensions" of the system. At the same time, it is known that the critical percolation indices are universal for systems in high dimensions [*Hara and Slade*, 1990] and trees are a simple model for infinite dimensional systems [*Albert and Barabasi*, 2002]. Thus, one expects to see the same values of the critical indices when working with percolation on a tree. From this perspective, the fact that our critical exponents vary from basin to basin still needs to be understood.

### 7.2. Further Work

[66] In this study we have considered only the simplest clustering rules for river streams: two streams belong to the

same cluster if there is a connected path from one stream to another along the river network. This approach is patterned after percolation studies and allows for a straightforward treatment. It may result, however, in a situation when two streams belong to the same cluster despite the fact that the respective fluxes are not mixed yet: think of two short streams that merge with a spatially extended cluster at about the same time. Formulating a physically more appropriate set of clustering rules might yield more realistic results for a wealth of transport problems related to river networks.

[67] So far, we have investigated only dynamic trees that have the same set of sources as the corresponding static tree; doing so is equivalent to injecting a flux through the sources alone. We emphasize at this point that the present study formulates merely a conceptual model, rather than attempting to mimic the realistic dynamics of fluxes in river networks. Indeed, actual precipitation or seepage from groundwater corresponds to activating multiple internal nodes within the network, not only its sources. Moreover, it might happen that a flux of interest is injected exclusively into an internal node, e.g., an industrial pollutant from a plant or nutrient production from a local biotic activity. Such situations can be modeled by considering a dynamic tree whose sources sample the entire river network. More elaborate models along these lines are also left to further study.

[68] The flux propagation model used in this paper is highly idealized (constant speed) and it only allows for continuous downstream transport, while real fluxes can violate both of these assumptions. For instance, sediments can be routed intermittently, undergoing several periods of intervening storage before arrival at points downstream. In addition, there exist upstream extensions of surface flow into headwater valleys of zero order. We notice also that the flux velocity may depend on slope or other factors, thus violating our assumption of constant transport velocity. These as well as other extensions of the simple model considered herein can be incorporated, in principle, into our general framework. Doing so certainly constitutes an interesting avenue for future work. It remains, of course, to be seen whether or not any of these potential extensions affect the main conceptual and qualitative conclusions of this study.

[69] To construct a richer theoretical framework for envirodynamics on river networks one may also model the transport along real and synthetic networks by using Boolean delay equations (BDEs) [*Dee and Ghil*, 1984; *Ghil and Mullhaupt*, 1985]. In BDEs, the discrete state variables describe the flux through the river branches; naturally, the rules for updating these variables inherit the child-parent relationship of the stream's static tree. The parent variables are updated based on the values of the children variables, after delays that correspond to the time it takes the flux to propagate from a child to its parent. *Ghil et al.* [2008] recently reviewed BDEs and their applications to climate and earthquake modeling. We expect such models to shed further light on the complex and important problems of transport on river networks.

## Appendix A: Hierarchical Aggregation and Cluster Dynamics: Examples

[70] Among the many instances of the general aggregation scheme of section 4, we mention here the following three.

[71] 1. In the site percolation process on an $L \times L$ lattice, the initial $N = L^2$ particles correspond to the sites of the lattice, while clusters correspond to connected patches of occupied sites that are formed during the percolation process [*Albert and Barabasi*, 2002; *Zaliapin et al.*, 2005]. The same scheme can be applied to bond percolation, as well as to percolation on grids in higher dimensions.

[72] 2. Elastic billiard on a rectangular table can be used to model gas dynamics in two dimensions (2-D). Here the initial particles are the $N$ billiard balls (gas molecules) at time $t = 0$. Each of the balls is assigned an initial position and velocity. The clusters at time $\Delta$ are formed by balls that have collided during the time interval $[0, \Delta]$ [*Gabrielov et al.*, 2008]. Formally, two balls are called $\Delta$ neighbors if they collided during the time interval $[0, \Delta]$. Each connected component of this neighbor relation is called a $\Delta$ cluster. Notice that within an arbitrary $\Delta$ cluster each ball has collided with at least one other ball during the time interval $[0, \Delta]$. In other words, a $\Delta$ cluster is a group of balls that have affected each other's dynamics during the time interval of duration $\Delta$. The mass of each cluster is simply the total number of balls within that cluster. Upon many collisions of the balls, the whole system will be composed of clusters of different sizes. As time evolves, the number of clusters will decrease and their mass increase.

[73] The same scheme can be applied to a system of particles that interact according to some potential $U(x)$. *Bogolyubov* [1960] suggested that when the interaction of particles is restricted to the near field, the system can be decomposed into finite clusters so that during some random interval of time, each cluster moves independently of other clusters as a finite dimensional dynamical system. After this time interval, the system can be decomposed again into other dynamically independent clusters and so on. This type of dynamics is called cluster dynamics and *Sinai* [1974] showed analytically that it exists in a one-dimensional (1-D) system of statistical mechanics. Numerical results of *Gabrielov et al.* [2008] describe the presence and various properties of cluster dynamics in a 2-D system of hard balls.

[74] In the metric setup of section 4.2 for the billiard dynamics, the space $\mathbb{S}$ is the set of $N$ billiard balls and the distance function $d(a, b)$ equals the time before the first collision of the balls $a$ and $b$. Naturally, this distance depends on the initial positions and velocities of the two balls $a$ and $b$, but it is also affected by the global billiard dynamics: our two balls may be set to collide at a given time $t^*$ in the absence of other balls, but may be hit by some other ball at time $t < t^*$, thus postponing the collision. The ultrametric distance $u(a, b)$ equals the time before both $a$ and $b$ belong to the same dynamic cluster. It is readily seen that $u(a, b) \leq d(a, b)$ since two balls do not have to collide to be within the same cluster; yet a collision necessarily puts them into the same cluster.

[75] 3. Probably the best known application of hierarchical aggregation is in constructing phylogenetic trees that describe the evolutionary relationships among biological species [*Maher*, 2002]. Here, a node corresponds to a set of species. Two species are connected if they have a direct common ancestor; the link length from a species to its direct ancestor equals the time it took to develop the descendant species from that ancestor.

[76] **Acknowledgments.** We thank Paola Passalacqua for helping with the river network extraction. The Grigno and Tirso digital elevation model (DEM) data were provided by the group of Andrea Rinaldo at the University of Padova, Italy. We are grateful to Mike Church, Colin Stark, and four anonymous referees for insightful reviews that substantially improved our earlier manuscript. This work is part of NSF's CMG collaborative research project "Envirodynamics on River Networks," supported by grants EAR-0934628 (to E.F.G.), EAR-0934426 (to M.G.), and EAR-0934871 (to I.Z.). Furthermore, E.F.G.'s research was partly supported by the National Center for Earth-surface Dynamics (NCED), a Science and Technology Center funded by NSF under agreement EAR-0120914, as well as by NSF grants EAR-0824084 and EAR-0835789; M.G.'s research was partly supported by DOE grant DE-FG02-07ER64439 from the Climate Change Prediction Program (CCPP); and I.Z.'s research was partly supported by DOE grant DE-FG02-07ER64440 from the CCPP and by NSF grant ATM-0620838.

## References

Albert, R., and A.-L. Barabasi (2002), Statistical mechanics of complex networks, *Rev. Mod. Phys.*, *74*, 47–97.

Barrat, A., M. Barthélemy, and A. Vespignani (2008), *Dynamical Processes on Complex Networks*, Cambridge Univ. Press, New York.

Benda, L., N. Leroy, D. Miller, T. Dunne, G. Reeves, G. Pess, and M. Pollock (2004a), The network dynamics hypothesis: How channel networks structure river habitat, *Bioscience*, *54*(5), 413–427.

Benda, L., K. Andras, D. Miller, and P. Bigelow (2004b), Confluence effects in rivers: Interactions of basin scale, network geometry, and disturbance regimes, *Water Resour. Res.*, *40*, W05402, doi:10.1029/2003WR002583.

Bertoin, J. (2006), *Random Fragmentation and Coagulation Processes*, Cambridge Univ. Press, New York.

Bogolyubov, N. N. (1960), Problems of dynamic theory in statistical physics, *Rep. AEC-tr-3852*, Fed. Publ. House for Tech.-Theor. Lit., Moscow.

Costa-Gabral, M. C., and S. J. Burges (1994), Digital elevation model neworks (DEMON): A model flow over hillslopes for computation of contributing and dispersal areas, *Water Resour. Res.*, *30*, 1681–1692.

Dee, D., and M. Ghil (1984), Boolean difference equations, I: Formulation and dynamic behavior, *SIAM J. Appl. Math.*, *44*, 111–126.

Dodds, P. S., and D. H. Rothman (2000), Scaling, Universality, and Geomorphology, *Annu. Rev. Earth Planet. Sci.*, *28*, 571–610, doi:10.1146/annurev.earth.28.1.571.

Dorogovtsev, S. N., and J. F. F. Mendes (2002), Evolution of networks, *Adv. Phys.*, *51*, 1079–1187.

Durrett, R. (2007), *Random Graph Dynamics*, Cambridge Univ. Press, New York.

Gabrielov, A., V. Keilis-Borok, Y. Sinai, and I. Zaliapin (2008), Statistical properties of the cluster dynamics of the systems of statistical mechanics, in *ESI Lecture Notes in Mathematics and Physics: Boltzmann's Legacy*, edited by G. Gallavotti et al., pp. 203–216, Eur. Math. Soc., Zurich.

Ghil, M., and A. P. Mullhaupt (1985), Boolean delay equations. II: Periodic and aperiodic solutions, *J. Stat. Phys.*, *41*, 125–173.

Ghil, M., I. Zaliapin, and B. Coluzzi (2008), Boolean delay equations: A simple way of looking at complex systems, *Physica D*, *237*, 2967–2986.

Giannoni, F., G. Roth, and R. Rudari (2005), A procedure for drainage network identification from geomorphology and its application to the prediction of the hydrologic response, *Adv. Water Resour.*, *28*, 567–581.

Gupta, V. K., and O. Mesa (1988), Runoff generation and hydrologic response via channel network geomorphology—Recent progress and open problems, *J. Hydrol.*, *102*, 3–28.

Guzzetti, F., C. P. Stark, and P. Salvati (2005), Evaluation of flood and landslide risk to the population of Italy, *Environ. Manage.*, *36*, 15–36.

Hancock, G. R., and K. G. Evans (2006), Channel head location and characteristics using digital elevation models, *Earth Surf. Processes Landforms*, *31*, 809–826.

Hara, T., and G. Slade (1990), Mean-field critical behaviour for percolation in high dimensions, *Commun. Math. Phys.*, *128*, 333–391.

Horton, R. E. (1945), Erosional development of streams and their drainage basins: Hydrophysical approach to quantitative morphology, *Geol. Soc. Am. Bull.*, *56*, 275–370.

Jarvis, R. S., and M. J. Woldenberg (Eds.) (1984), *River Networks, Benchmark Pap. Geol.*, vol. 80, Hutchinson Ross, Stroudsburg, Pa.

Keilis-Borok, V. I., and A. A. Soloviev (Eds.) (2003), *Nonlinear Dynamics of the Lithosphere and Earthquake Prediction*, 337 pp., Springer, Berlin.

Kiffney, P. M., C. M. Greene, J. E. Hall, and J. R. Davies (2006), Tributary streams create spatial discontinuities in habitat, biological productivity, and diversity in mainstream rivers, *Can. J. Fish. Aquat. Sci.*, *63*, 2518–2530, doi:10.1139/F06-138.

Kirkby, M. J. (1976), Tests of the random network model, and its application to basin hydrology, *Earth Surf. Processes*, *1*, 197–212.

Lashermes, B., E. Foufoula-Georgiou, and W. E. Dietrich (2007), Channel network extraction from high resolution topography using wavelets, *Geophys. Res. Lett.*, *34*, L23S04, doi:10.1029/2007GL031140.

Leyvraz, F. (2003), Scaling theory and exactly solved models in the kinetics of irreversible aggregation, *Phys. Rep.*, *383*(2-3), 95–212.

Lowe, W. H., G. E. Likens, and B. J. Cosentino (2006), Self-organization in streams: The relationship between movement behavior and body condition in a headwater salamander, *Freshwater Biol.*, *51*, 2052–2062, doi:10.1111/j.1365-2427.2006.01635.x.

Maher, B. A. (2002), Uprooting the tree of life, *The Scientist*, *16*(18), 26.

McConnell, M., and V. Gupta (2008), A proof of the Horton law of stream numbers for the Tokunaga model of river networks, *Fractals*, *16*, 227–233.

Montgomery, D. R., and W. E. Dietrich (1989), Source areas, drainage density, and channel initiation, *Water Resour. Res.*, *25*, 1907–1918.

Montgomery, D. R., and E. Foufoula-Georgiou (1993), Channel network source representation using digital elevation models, *Water Resour. Res.*, *29*, 3925–3934.

Molchan, G., O. Dmitrieva, I. Rotwain, and J. Dewey (1990), Statistical analysis of the results of earthquake prediction, based on bursts of aftershocks, *Phys. Earth Planet. Inter.*, *61*, 128–139.

Muneepeerakul, R., S. A. Levin, A. Rinaldo, and I. Rodriguez-Iturbe (2007), On biodiversity in river networks: A trade-off metapopulation model and comparative analysis, *Water Resour. Res.*, *43*, W07426, doi:10.1029/2006WR005857.

Newman, M. E. J. (2003), The structure and function of complex networks, *SIAM Rev.*, *45*, 167–256.

Newman, M. E. J., A.-L. Barabasi, and D. J. Watts (2006), *The Structure and Dynamics of Networks*, Princeton Univ. Press, Princeton, N. J.

Newman, W. I., D. L. Turcotte, and A. M. Gabrielov (1997), Fractal trees with side branching, *Fractals*, *5*, 603–614.

Passalacqua, P., T. Do Trung, E. Foufoula-Georgiou, G. Sapiro, and W. E. Dietrich (2010), A geometric framework for channel network extraction from lidar: Nonlinear diffusion and geodesic paths, *J. Geophys. Res.*, *115*, F01002, doi:10.1029/2009JF001254.

Peckham, S. (1995), New results for self-similar trees with applications to river networks, *Water Resour. Res.*, *31*, 1023–1029.

Peckham, S., and V. Gupta (1999), A reformulation of Horton's laws for large river networks in terms of statistical self-similarity, *Water Resour. Res.*, *35*, 2763–2777.

Pinna, M., A. Fonnesu, F. Sangiorgio, and A. Basset (2004), Influence of summer drought on spatial patterns of resource availability and detritus processing in Mediterranean stream sub-basins (Sardinia, Italy), *Int. Rev. Hydrobiol.*, *89*(5-6), 484–499.

Power, M. E., and W. E. Dietrich (2002), Food webs in river networks, *Ecol. Res.*, *17*, 451–471.

Rammal, R., G. Toulouse, and M. A. Virasoro (1986) Ultrametricity for physicists, *Rev. Mod. Phys.*, *58*, 765–788.

Rice, S., and M. Church (1998), Grain size along two gravel-bed rivers: Statistical variation, spatial pattern and sediment links, *Earth Surf. Processes Landforms*, *23*, 345–363.

Rice, S. P., R. I. Ferguson, and T. B. Hoey (2006), Tributary control of physical heterogeneity and biological diversity at river confluences, *Can. J. Fish. Aquat. Sci.*, *63*, 2553–2556, doi:10.1139/F06-145.

Rodriguez-Iturbe, I., and A. Rinaldo (1997), *Fractal River Networks: Chance and Self-Organization*, Cambridge Univ. Press, New York.

Rodriguez-Iturbe, I., and J. B. Valdes (1979), The geomorphologic structure of hydrologic response, *Water Resour. Res.*, *15*, 1409–1420, doi:10.1029/WR015i006p01409.

Rodriguez-Iturbe, I., E. Ijjasz-Vasquez, R. L. Bras, and D. G. Tarboton (1992), Power law distributions of mass and energy in river basins, *Water Resour. Res.*, *28*, 1089–1093.

Rotwain, I., V. Keilis-Borok, and L. Botvina (1997), Premonitory transformation of steel fracturing and seismicity, *Phys. Earth Planet. Inter.*, *101*, 61–71.

Schikhof, W. H. (2007), *Ultrametric Calculus: An Introduction to P-Adic Analysis*, 318 pp., Cambridge Univ. Press, New York.

Shreve, R. L. (1966), Statistical law of stream numbers, *J. Geol.*, *74*, 17–37.

Sklar, L. S., W. E. Dietrich, E. Foufoula-Georgiou, B. Lashermes, and D. Bellugi (2006), Do gravel bed river size distributions record channel network structure?, *Water Resour. Res.*, *42*, W06D18, doi:10.1029/2006WR005035.

Sinai, Ya. G. (1972), Construction of the dynamics for one-dimensional systems of statistical mechanics, *Theor. Math. Fiz.*, *11*(12), 248–258. (*Theor. Math. Phys.*, Engl. Transl., *11*, 487–494.)

Sinai, Ya. G. (1974), Construction of cluster dynamics for dynamical systems of statistical mechanics, *Moscow Univ. Math. Bull.*, *29*, 124–129.

Sposito, G. (Ed.) (1998), *Scale Dependence and Scale Invariance in Hydrology*, Cambridge Univ. Press, New York.

Stauffer, D., and A. Aharony (1994), *Introduction to Percolation Theory*, 2nd ed., Taylor and Francis, London.

Strahler, A. N. (1957), Quantitative analysis of watershed geomorphology, *Eos Trans., AGU*, *38*, 913–920.

Stewart-Koster, B., M. J. Kennard, B. D. Harch, F. Sheldon, A. H. Arthington, and B. J. Pusey (2007), Partitioning the variation in stream fish assemblages within a spatio-temporal hierarchy, *Mar. Freshwater Res.*, *58*, 675–686.

Surkan, A. J. (1969), Synthetic hydrographs: Effects of network geometry, *Water Resour. Res.*, *5*, 112–128.

Tarboton, D. R., R. L. Bras, and I. Rodriguez-Iturbe (1991), On the extraction of channel networks from digital elevation data, *Hydrol. Processes*, *5*, 81–100.

Tokunaga, E. (1978), Consideration on the composition of drainage networks and their evolution, *Geogr. Rep. Tokyo Metro. Univ.*, *13*, 1–27.

Veitzer, S., and V. K. Gupta (2000), Random self-similar river networks and derivations of generalized Horton laws in terms of statistical simple scaling, *Water Resour. Res.*, *36*, 1033–1048.

Wakeley, J. (2009), *Coalescent Theory*, Roberts and Company, Greenwood Village, Colo.

Wohl, E., D. Cooper, L. Poff, F. Rahel, D. Staley, and D. Winters (2007), Assessment of stream ecosystem function and sensitivity in the Bighorn National Forest, *Environ. Manage.*, *40*, 282–302, doi:10.1007/s00267-006-0168-z.

Zaliapin, I., H. Wong, and A. Gabrielov (2005), Inverse cascade in percolation model: Hierarchical description of time-dependent scaling, *Phys. Rev. E*, *71*, 066118, doi:10.1103/PhysRevE.71.066118.

E. Foufoula-Georgiou, Saint Anthony Falls Laboratory and National Center for Earth-surface Dynamics, Department of Civil Engineering, University of Minnesota, Minneapolis, MN 55414, USA. (efi@umn.edu)

M. Ghil, Department of Atmospheric and Oceanic Sciences, University of California, Los Angeles, CA 90095, USA. (ghil@atmos.ucla.edu)

I. Zaliapin, Department of Mathematics and Statistics, University of Nevada, Reno, NV 89557, USA. (zal@unr.edu)